Production of Highly Polarized Positron Beams via Helicity Transfer from Polarized Electrons in a Strong Laser Field

Yan-Fei Li[1,*] Yue-Yue Chen,[2,†] Wei-Min Wang[3,4,5] and Hua-Si Hu[1,‡]

[1]*Department of Nuclear Science and Technology, School of Energy and Power Engineering, Xi'an Jiaotong University, Xi'an 710049, China*
[2]*Department of Physics, Shanghai Normal University, Shanghai 200234, China*
[3]*Department of Physics and Beijing Key Laboratory of Opto-electronic Functional Materials and Micro-nano Devices, Renmin University of China, Beijing 100872, China*
[4]*Beijing National Laboratory for Condensed Matter Physics, Institute of Physics, CAS, Beijing 100190, China*
[5]*Collaborative Innovation Center of IFSA (CICIFSA), Shanghai Jiao Tong University, Shanghai 200240, China*

The production of a highly polarized positron beam via nonlinear Breit-Wheeler processes during the interaction of an ultraintense circularly polarized laser pulse with a longitudinally spin-polarized ultra-relativistic electron beam is investigated theoretically. A new Monte Carlo method employing fully spin-resolved quantum probabilities is developed under the local constant field approximation to include three-dimensional polarization effects in strong laser fields. The produced positrons are longitudinally polarized through polarization transferred from the polarized electrons by the medium of high-energy photons. The polarization transfer efficiency can approach 100% for the energetic positrons moving at smaller deflection angles. This method simplifies the postselection procedure to generate high-quality positron beams in further applications. In a feasible scenario, a highly polarized (40%–65%), intense (10^5–10^6/bunch), collimated (5–70 mrad) positron beam can be obtained in a femtosecond timescale. The longitudinally polarized positron sources are desirable for applications in high-energy physics and material science.

As a powerful probe, spin-polarized positrons play irreplaceable roles in fundamental physical studies and applications. Low-energy (eV to keV) positrons can be utilized to probe the surface [1] and bulk [2] magnetism of materials [3]. High-energy (GeV to hundreds of GeV) positrons improve the sensitivity of the two photon effect experiments [4], and are essential for an unambiguous determination of the nucleon structure [5], testing the standard model and searching for new physics beyond it [6]. The proposed international linear collider (ILC) [7] is designed for discovering physics beyond the standard model with polarized electrons and positrons at energies of 500 GeV. The positrons are required with polarization more than 30%, density $\sim 10^{10} e^+$/bunch, and beam size in nm scale at the interaction point [8].

Polarized positrons can be obtained from beta decays of specific radioisotopes [9]. However, the large angular divergence, large energy spread and low intensity of the positron beam from beta decays limit its applications. Storage rings can be used to polarize positrons via Sokolov-Ternorv effect [10], but this time consuming mechanism brings forward rigorous requirements on space-scale and layout to experiments. Nowadays, two methods based on the Bethe-Heitler (BH) process are extensively adopted to produce polarized positrons. One is the photon-solid interaction, with circularly polarized

(CP) γ rays generated by linear Compton scattering between CP lasers with unpolarized electrons [11], or by synchrotron radiation of unpolarized electrons moving in helical undulators [12]. The other is the electron-solid interaction, with longitudinally spin-polarized (LSP) electrons [13]. However, the energy conversion efficiency from initial electrons to photons in the former way is rather low due to the low fundamental parameter $K(\ll 1)$ of the undulator [14]. The latter suffers from high depolarization rates and large angular divergences due to multiple scattering in the Coulomb field of nuclei (Mott scattering) [15,16], restricting the target thickness to be $\lesssim 0.2 L_{\rm rad}$ ($L_{\rm rad}$ is the radiation length typically in several mm [17]), and consequently limiting the total yield of positrons to $\lesssim 0.01 e^+/e^-$ [13,15,18]. Currently, the state-of-the-art techniques can provide polarized positron beams with polarization 30%–80%, density $\sim 10^4 e^+$/bunch, and angular divergence more than 20° [11–13,19]. Challenging technology upgrades are still needed to meet the experimental requirements above [7,8].

Recent progress in development of ultraintense laser system [20] has stimulated the interest in producing polarized positrons with strong laser field [21–30]. Since the fierce laser-induced pair production is free from Mott scattering and implemented in nonlinear QED regime ($K \gg 1$), the produced positrons are expected to be a

desirable alternative along with outstanding features similar with other laser-driven sources [14,31–33], such as high brilliance [34,35], ultrashort duration [36], low angular divergence [37], and high beam intensity [38,39]. For instance, an asymmetric two-color laser field can produce polarized positrons with a polarization degree of around 60%, angular divergence of ~74 mrad and yield of ~$0.01e^+/e^-$ [27]. Meanwhile, a fine-tuning small ellipticity of a laser pulse results in an angular dependent polarization of created positrons [28]. However, all suggested schemes are only able to deliver positrons with transverse polarization, while longitudinal polarization is employed in most applications. To solve this problem, a polarization rotator has to be applied under the risk of particle-amount plummeting since the rotator works for monoenergetic particles with a limited energy range [40,41]. Besides, the effect of photon polarization on pair production is not considered in these schemes, the impact of which especially on pair polarization is crucial as shown below.

In this Letter, we investigate theoretically the feasibility of production of a longitudinally polarized ultrarelativistic positron beam via the interaction of a *CP* ultraintense laser pulse with a LSP counterpropagating ultrarelativistic electron beam in the quantum radiation-dominated regime [42], see Fig. 1. Two steps contribute to the positron polarization. First, circularly polarized photons are radiated during nonlinear Compton scattering (NCS) of a CP laser pulse with a LSP electron beam [26]. Then, the helicity of the high-energy photons transfers to electron-positron pairs via nonlinear Breit-Wheeler (NBW) pair production process. To investigate the helicity transfer and photon polarization effects during NCS and NBW, a new Monte Carlo method, involving all polarization effects of electron (positron) and photon in realistic, tightly focused laser fields, is developed firstly for simulations. Our simulation shows, under the external electromagnetic fields, a highly longitudinally polarized positron beam can be produced with a small angular divergence and high intensity.
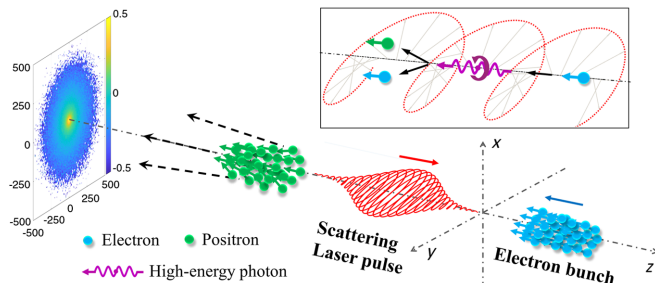

FIG. 1. Scenarios of generation of a LSP ultrarelativistic positron beam via an ultraintense laser pulse head-on colliding with a counterpropagating LSP electron beam. First, longitudinal polarization (helicity) is transferred from electron to photon during NCS, then, from high-energy photon to positron through NBW process, as shown in the inset.

Our Monte Carlo method [43–49], treats photon emission and pair production quantum mechanically, and describes the electron (positron) spin-resolved dynamics semiclassically. In particular, photon emission and pair production are conducted by the common statistical event generators, based on quantum probabilities derived via the QED operator method in the local constant field approximation (LCFA) [45], to determine whether or not a photon emission or pair production occurs at each simulation step (see the details in the Supplemental Material [50]). The LCFA is valid in an ultraintense laser field, with the invariant laser field parameter $a_0 \equiv eE_0/(m\omega_0) \gg 1$, where the formation length of radiation and pair production are far shorter than the laser wavelength and the typical size of the electron (positron) trajectory [43,45,51]. Here, E_0 is the laser field amplitude, ω_0 is the laser frequency, and $e(>0), m$ are the electron charge and mass, respectively. Relativistic units $\hbar = c = 1$ are used throughout.

Moreover, our Monte Carlo algorithm features the description of polarization effects. In contrast with the previous Monte Carlo methods related to particular observable of interest [22,23,25–28], our new method extends the simulation capacity from solving one-dimensional polarization problem to three-dimensional, by choosing the instantaneous spin quantization axis (SQA) according to the properties of the scattering process [52] instead of the detector (e.g., the direction of magnetic field in the rest frame [22,23,25,27,28] or the direction of initial electron polarization [26]). The shortcomings of the previous methods stemming from neglecting the phase relation between the two components of the spinor can be overcome [50]. Meanwhile, since photon polarization significantly affects pair production rate ($\geq 10\%$, investigated recently in [53,54]) and positron polarization (~60%, see [50]), we improved the Monte Carlo method [27,28,46,47,49,53,54] by employing the photon-polarization- and pair-spin-resolved pair production probability applicable to strong laser fields [45], and therefore provide a more thorough way to simulate the NBW process.

The details of our Monte Carlo algorithm are elaborated as follow. The electron (positron) spin jumps into one of its basis states defined with respect to SQA in each time step, regardless whether a photon emission happens or not. The spin-resolved radiation probability can be written in form of $W_R = a + \mathbf{S}_f^R \cdot \mathbf{b}$ [22,50]. When a photon emitted, the SQA is chosen to be along $\mathbf{b}$. The final polarization vector $\mathbf{S}_f^R$ is decided with a stochastic procedure: if $W_R^+/(W_R^+ + W_R^-) > R_a$, $\mathbf{S}_f^R = +\mathbf{b}/|\mathbf{b}|$; otherwise $\mathbf{S}_f^R = -\mathbf{b}/|\mathbf{b}|$. Here, R_a is a random number in [0,1]; and $W_R^{+,-}$ are the probabilities calculated by taking $\mathbf{S}_f^R$ as $\pm\mathbf{b}/|\mathbf{b}|$, respectively. When a photon emission does not occur, the electron (positron) spin should also change quantum mechanically [49]. The probability for no photon emission takes the form of $W_{NR} = \frac{1}{2}(c + \mathbf{S}_f^{NR} \cdot \mathbf{d})$ [49], and

the SQA is along **d**. The final polarization vector $\mathbf{S}_f^{NR}$ is decided with probability W_{NR} and the stochastic procedure mentioned above. Here, a, **b**, c, and **d** are functions of emitted photon energy, field strength and etc. [50]. The polarization of the emitted photon is determined with a same algorithm [26,50].

Similarly, the polarization vectors of a newly created pair is calculated with spin-resolved probability of [45]

$$\frac{d^2 W_{\text{pair}}}{d\varepsilon_+ dt} = \frac{C_P}{2}(h + \mathbf{S}_+ \cdot \mathbf{j}), \qquad (1)$$

$$h = \left(\frac{\omega_\gamma^2}{\varepsilon_+ \varepsilon_-} - 2\right) K_{2/3}(\rho) + \text{Int}K_{1/3}(\rho) - \xi_3 K_{2/3}(\rho), \qquad (2)$$

$$\mathbf{j} = -\xi_1 \frac{\omega_\gamma}{\varepsilon_-} K_{1/3}(\rho) \hat{\mathbf{e}}_1 - K_{1/3}(\rho) \left(\frac{\omega_\gamma}{\varepsilon_+} - \xi_3 \frac{\omega_\gamma}{\varepsilon_-}\right) \hat{\mathbf{e}}_2$$

$$+ \xi_2 \left[\frac{\omega_\gamma}{\varepsilon_+} \text{Int}K_{1/3}(\rho) + \frac{\varepsilon_+^2 - \varepsilon_-^2}{\varepsilon_+ \varepsilon_-} K_{2/3}(\rho)\right] \hat{\mathbf{e}}_v, \qquad (3)$$

where $C_p = \alpha m^2/(\sqrt{3}\pi\omega_\gamma)$, ω_γ, ε_+, and ε_- are the energies of the photon, positron, and electron, respectively, with $\omega_\gamma = \varepsilon_+ + \varepsilon_-$, $\rho = 2\omega_\gamma^2/(3\chi_\gamma \varepsilon_+ \varepsilon_-)$, $\text{Int}K_{1/3}(p) \equiv \int_p^\infty dz K_{1/3}(z)$, K_n is the n-order modified Bessel function of the second kind, $\boldsymbol{\xi} = (\xi_1, \xi_2, \xi_3)$ refers to the photon polarization vector with ξ_i ($i = 1, 2, 3$) being the Stokes parameters defined with respect to the axes of $\hat{\mathbf{e}}_1$ and $\hat{\mathbf{e}}_2$ [16]. $\hat{\mathbf{e}}_1$ is the unit vector along the direction of the transverse component of acceleration, $\hat{\mathbf{e}}_2 = \hat{\mathbf{e}}_v \times \hat{\mathbf{e}}_1$ with $\hat{\mathbf{e}}_v$ as the unit vector along positron velocity. Quantum parameter is defined as $\chi_{\gamma,e} \equiv |e|\sqrt{-(F_{\mu v}p^v)^2}/m^3$ with p^v the four-vector of photon or electron (positron) momentum. The spin state of the newborn positron is set as one of the two states: $\mathbf{S}_+ = \pm\mathbf{j}/|\mathbf{j}|$, via stochastic procedure. The spin state of produced electron is also obtained with Eq. (1), through replacing ε_+, ε_- and $\mathbf{S}_+$ with ε_-, ε_+ and $\mathbf{S}_-$, respectively.

Between quantum events, the electron (positron) dynamics in the ultraintense laser field are described by Lorenz equations classically, and the spin precession is governed by the Thomas-Bargmann-Michel-Telegdi equation [55]. The detailed description and accuracy of the method are exhibited in the Supplemental Material [50], which includes Refs. [56,57].

A typical simulation result for production of polarized positrons with a realistic tightly focused Gaussian laser pulse [58] is shown in Fig. 2. The peak laser intensity is $I_0 \approx 2.75 \times 10^{22}$ W/cm^2 ($a_0 = 100\sqrt{2}$), pulse duration (the full width at half maximum, FWHM) $\tau = 5T_0$ with T_0 the period, wavelength $\lambda = 1$ μm, and focal radius $w_0 = 5\lambda$. The colliding electron bunch is set with typical parameters of laser-accelerated electron source [31,59,60], for a potential compact all-optical facility. $N_e = 9.6 \times 10^5$
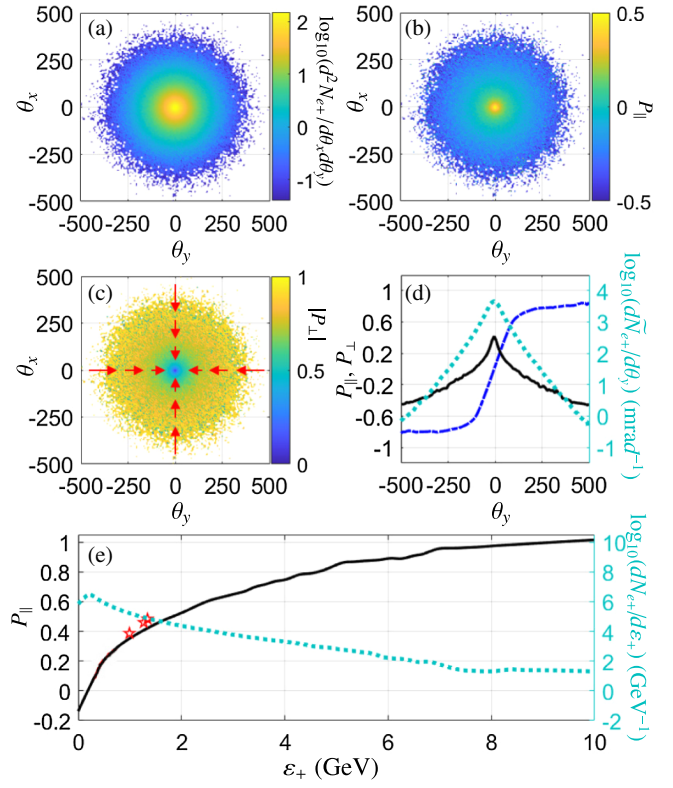

FIG. 2. Angular distribution of number density $\log_{10}(d^2 N_{e+}/d\theta_x d\theta_y)$ (mrad^{-2}) (a), Longitudinal polarization $P_\parallel = -\bar{S}_z$ (b), and transverse polarization degree $|P_\perp| = \sqrt{\bar{S}_x^2 + \bar{S}_y^2}$ for $P_\perp = (\bar{S}_x, \bar{S}_y)$ (c), vs positron deflection angles of $\theta_x = p_x/p_z$ and $\theta_y = p_y/p_z$. (d): $P_\parallel$ (black-solid), $P_\perp$ (blue dash-dotted), and number density $\log_{10}(d\tilde{N}_{e+}/d\theta_y)$ (mrad^{-1}) (cyan-dotted) vs θ_y, for positrons with θ_x into $[-20, 20]$. Here, $d\tilde{N}_{e+}/d\theta_y = \int_{-20}^{20} d^2 N_{e+}/(d\theta_x d\theta_y)d\theta_x$; $\bar{S}_x = 0$ after averaged over $[-20, 20]$, $P_\perp = \bar{S}_y$. (e): $P_\parallel$ (black-solid line) and $\log_{10}(dN_{e+}/d\varepsilon_+)$ (GeV^{-1}) (cyan dotted) vs positron-energy ε_+. The red stars indicate positrons with deflection angle $\theta = \sqrt{\theta_x^2 + \theta_y^2}$ within 5, 10, and 20 mrad, from right to left, respectively.

electrons are uniformly distributed longitudinally and normally distributed transversely in a cylindrical form at length of $L_e = 6\lambda$ and standard deviation of $\sigma_{x,y} = 0.6\lambda$. The initial mean kinetic energy is $\varepsilon_i = 10$ GeV (correspondingly $\chi_{\gamma,e}^{\max} \approx 9.5$ for substantial high-energy photon emissions and pair productions), the energy spread $\Delta\varepsilon_i/\varepsilon_i = 6\%$, and the angular divergence $\Delta\theta = 0.2$ mrad. For the optimal description on polarization transferring, the initial electrons are set to be 100% longitudinally polarized, i.e., $S_z = -1$ (the feasibility of our scheme for a more relaxed requirement is shown in [50]). Such polarized electron bunches can be obtained via laser wakefield acceleration with further radiative polarization [22], or laser-wakefield acceleration of prepolarized electrons

[21,61,62]. Alternatively, highly polarized (>80%) ultra-relativistic electrons can also be generated by radiative polarization in storage ring [63], or extracting polarized electrons directly from polarized photocathodes [6,64].

The produced positrons mainly concentrate in the center of the angular distribution with angular divergence around 70 mrad, see Fig. 2(a). The total yield of positrons is 1.17 e^+/e^-. Positrons are longitudinally polarized with $P_\parallel > 0$ for $\theta \lesssim 100$ mrad and $P_\parallel < 0$ for $\theta \gtrsim 100$ mrad, as shown in Fig. 2(b). For more intuitive features, one can refer to the angular distribution of density and polarization for positrons at $\theta_x \in [-20, 20]$ mrad, see Fig. 2(d). The positron density dramatically declines with the increase of deflection angle; and $P_\parallel$ decreases with the rising of $|\theta_y|$, from 43% to −45%. Moreover, $P_\parallel$ is proportional to positron energy, similar with that in BH process [18], see Fig. 2(e), but the positron yield is two orders higher. Higher polarization can be achieved by using the post-energy-selection technique [11,13]. For instance, positrons with energy higher than 2, 4, 6, and 8 GeV can be selected in a spectrometer consisting of a pair of dipole magnets, leading to 62.5%, 81.9%, 91.8%, and 98.6% polarization, and $0.019 e^+/e^-$, $0.002 e^+/e^-$, $1.51 \times 10^{-4} e^+/e^-$, and $5.21 \times 10^{-6} e^+/e^-$ yields, respectively. The positron energy ranges from MeV to 10 GeV with a mean value of 0.345 GeV, see Fig. 2(e). The maximal energy conversion efficiency $\epsilon_{max} \approx 1$ and the average energy conversion efficiency $\bar{\epsilon} \approx 0.034$, much higher than that in BH process ($\epsilon_{max} \approx 0.05$ and $\bar{\epsilon} \approx 0.003$ for photons from linear Compton scattering [11], and $\epsilon_{max} \approx 2 \times 10^{-4}$ and $\bar{\epsilon} \approx 4 \times 10^{-5}$ for photons emitted from a electron beam passing through a helical undulator [65]). Besides, the angle-dependent polarization distribution provides a more feasible way to improve polarization by dropping off positrons with higher θ via angle-selection technique [66]. For instance, after sending positrons through a straight long chamber (the so-called collimator [67]), the polarization of the positrons within 5, 10, and 20 mrad, can reach to 48.3%, 46.0%, and 38.7%, respectively. The small emittance (~0.02 mm mrad) is favorable for experimental operations such as beam injection [68].

The positrons have transverse polarization component $P_\perp$ directed radially pointing to the center of the beam-center axis, see Fig. 2(c). $P_\perp$ presents an angle dependence as well, i.e., $P_\perp > 0$ for $\theta_y > 0$, $P_\perp < 0$ for $\theta_y < 0$, and the amplitude $|P_\perp|$ increasing with the growing of $|\theta_y|$ from 0 to 80%, see Fig. 2(d). The radially polarized positron can be used as transversely polarized positrons by collecting positrons in a certain angle. The controlled polarization direction would be useful for testing detailed structure of the W^0 coupling [69].

The reason for generating polarized positrons is analyzed in Fig. 3. Processes of photon emission from NCS and pair production from NBW are investigated

separately in Figs. 3(a) and 3(b). Summing up the final spin states, the analytical estimations on circular polarization of photons and longitudinal polarization of positrons read,

$$\xi_2 = P_\parallel^i \frac{-u\mathrm{IntK}_{1/3}(u') + u(2 + u)\mathrm{K}_{2/3}(u')}{-(1 + u)\mathrm{IntK}_{1/3}(u') + 2(1 + u + u^2/2)\mathrm{K}_{2/3}(u')},$$
(4)

$$P_\parallel = -\xi_2 \frac{\omega_\gamma/\varepsilon_+ \mathrm{IntK}_{1/3}(\rho) + (\varepsilon_+^2 - \varepsilon_-^2)/(\varepsilon_+\varepsilon_-)\mathrm{K}_{1/3}(\rho)}{(\omega_\gamma^2/(\varepsilon_+\varepsilon_-) - 2)\mathrm{K}_{2/3}(\rho) + \mathrm{IntK}_{1/3}(\rho) - \xi_3\mathrm{K}_{2/3}(\rho)},$$
(5)

where, $P_\parallel^i$ is the initial electron polarization, $u = \delta_\gamma(1 - \delta_\gamma)$, $u' = 2u/3\chi_e$. Clearly, $P_\parallel = 0$, when the photon polarization is averaged. The investigation of helicity transfer is off the limit for previous studies [27,28]. The numerical results excluding RR effect, in Figs. 3(a) and 3(b), are in coincidence with the analytical ones, with differences mainly coming from the variety of χ_e (χ_γ) for photons (positrons) created at diverse points in a laser pulse, and [for Fig. 3(b)] from the asymmetry of electromagnetic field experienced by positrons. When radiation reaction is included, electron (positron) looses energy rapidly. The overlapping of photons emitted by electrons with lower
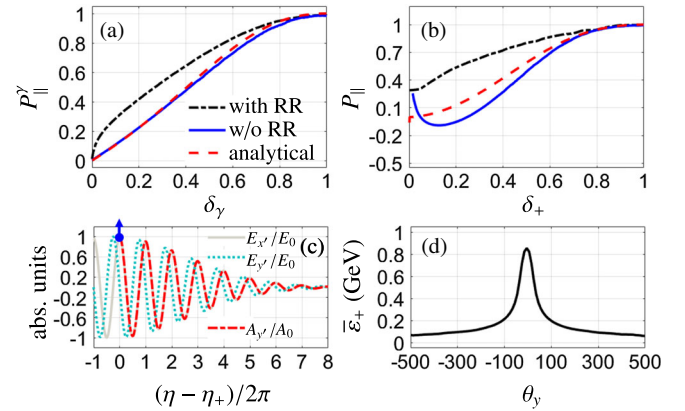

FIG. 3. (a) Circular polarization of photons $P_\parallel^\gamma = -\bar{\xi}_2$ vs the energy ratio parameter $\delta_\gamma = \omega_\gamma/\varepsilon_i$, from NCS. (b) Longitudinal polarization of positrons $P_\parallel$ vs the energy ratio parameter $\delta_+ = \varepsilon_+/\omega_\gamma$, from NBW of an initial photon beam with $\omega_\gamma = 10$ GeV: calculated numerically including (black-dash-dotted) or excluding radiation reaction (RR) effect (blue-solid, using the instantaneous $\chi_{e,\gamma}$ parameter), and analytically (red-dashed, employing the constant average value of $\bar{\chi}_e = 0.97$ or $\bar{\chi}_\gamma = 4.45$). The other parameters are the same with those in Fig. 2. (c) Normalized field components of $E_{x'}$ (grey solid), $E_{y'}$ (cyan dotted) and vector potential $A_{y'}$ (red dash dotted), vs laser phase $\eta - \eta_+$, with a positron created at η_+ (marked with blue point). The blue arrow represents the spin is antiparallel to $\hat{\mathbf{e}}_{y'}$. (d) Average energy $\bar{\varepsilon}_+$ vs θ_y, for positrons into $|\theta_x| \leq 20$ mrad. Panels (c) and (d) refer to the simulation case in Fig. 2.

energy ($\varepsilon_t < \varepsilon_i$) at higher δ_γ^t (i.e., higher $P_\parallel^\gamma$), with photons emitted by electrons with ε_i at δ_γ^i, at the condition of $\delta_\gamma^t \varepsilon_t = \delta_\gamma^i \varepsilon_i$, leads to a higher numerical polarization in the low energy part of $\delta_\gamma \ll 1$, in Fig. 3(a). Here, the suffix t indicates variables at evolution time t. Similarly, the overlapping of positrons created at higher δ_+^t (i.e., higher $P_\parallel$) experienced more energy-loss $\Delta\varepsilon_+^t$, with positrons created at lower δ_+^i experienced less energy-loss $\Delta\varepsilon_+^i$, at the condition of $\delta_+^t \omega_\gamma - \Delta\varepsilon_+^t = \delta_+^i \omega_\gamma - \Delta\varepsilon_+^i$, results in a higher numerical polarization in the low energy part of $\delta_+ \ll 1$, in Fig. 3(b). Above all, with helicity transferred from initial electron to photon, then to pair, we acquire the longitudinally polarized positrons in Fig. 2. The circular polarization of photon (positron) is proportional to its energy, and could approach 100% as ω_γ (ε_+) gets close to ε_i (ω_γ). Intuitively, the simultaneous energy and helicity transferring, from parent particle to newborn particle, causes the fact that higher helicity transfer efficiency would be accompanied by higher energy transfer efficiency.

When a $e^+ e^-$ pair is created at laser phase η_+, the final transverse momentum of the positron is $\mathbf{p}_\perp^f \approx \mathbf{p}_\perp^i - e\mathbf{A}(\eta_+)$, where $\mathbf{p}_\perp^i$ is the momentum inherited from the parent photon, and $\mathbf{A}(\eta_+)$ is the vector potential at production point. Since $\mathbf{p}_\perp^i$ is arbitrary due to the stochastic effects, $\overline{\mathbf{p}_\perp^\gamma} \approx 0$, and consequently the final transverse momenta of positrons should be $\mathbf{p}_\perp^f \approx -e\mathbf{A}(\eta_+)$. For simplicity, we rotate the laboratory coordinate system with respect to instantaneous electromagnetic field, such that $E_{x'} = E_0$, $E_{y'} = 0$, as shown in Fig. 3(c). In the new coordinate system, the final transverse momentum of a positron is antiparallel to the instantaneous $\hat{\mathbf{e}}_{y'}$. Since the pairs are mainly created by energetic photons with longitudinal polarization [50], the transverse polarization arises from the second term in Eq. (3), i.e., $K_{(1/3)}(\rho)\omega/\varepsilon_+ \hat{\mathbf{e}}_{y'}$, which also indicates polarization degree $|P_\perp|$ inversely proportional to energy. Therefore, positrons are produced with $\mathbf{p}_\perp^f$ antiparallel and $P_\perp$ parallel to $\hat{\mathbf{e}}_{y'}$ with the rotating of $\hat{\mathbf{e}}_{y'}$, i.e., the positrons are polarized radially, as shown in Fig. 3(c). Meanwhile, as deflection angle $\theta = p_\perp / p_\parallel \propto 1/\gamma_{e+}$, positrons with higher energy move at smaller deflection angles, as shown in Fig. 3(d). Above all, positrons moving closer to axis own higher energy, larger $P_\parallel$ but smaller $P_\perp$, as shown in Fig. 2(d).

The impacts of laser and electron beam parameters on the production of polarized positrons are investigated in [50]. The polarization of the produced LSP positrons is robust against the variation of pulse duration τ (3–10 T_0) and peak intensity a_0 ($50\sqrt{2}$–$150\sqrt{2}$) of the laser pulse, and initial average kinetic energy ε_i (5–10 GeV), angular divergence $\Delta\theta$ (0.2–5 mrad) and energy spread $\Delta\varepsilon_i/\varepsilon_i$ (0.06–0.2) of the electron beam. The scheme works very well even for a long electron bunch ($L_e = 100\lambda_0$) [6,70]. Generally speaking, larger a_0, τ, and ε_i are conducive to

higher yield and energy of photons emitted and positrons created, as $N_{e+} \propto N_\gamma \sim \alpha a_0 \tau / T_0$ and $\varepsilon_+ \sim \omega_\gamma \sim \chi_e \varepsilon_i \sim 10^{-6} a_0 \varepsilon_i^2 / m$ [42,43]. However, since large χ_e causes strong radiation loss and depolarization [45], a trade off exists for a_0, τ, and ε_i.

In conclusion, we have proposed a novel method on production of a highly polarized intense ultrarelativistic positron beam via PW laser pulses available recently, with the help of a newly developed Monte Carlo method. Through polarization transferring from the polarized electrons by the medium of high-energy photons, the positron polarization can be up to 100% of the initial electron polarization, with an unprecedented high yield and small angular divergence, making it a promising alternative source for future experimental facilities in high-energy physics, such as ILC. In a feasible scheme with a seed electron beam with polarization degree 80%, density 10^8/bunch and kinetic energy 10 GeV [21,59], a high-quality positron beam can be generated with polarization degree 40%, angle range 5 mrad, density 10^6/bunch and average energy 1.4 GeV. Given a possible ultrahigh-charge ($\sim$100 nC [38]) of electron beams, a positron beam density of 10^9–10^{10}/bunch is foreseeable. The yield and angular divergence of positron beam is increased and decreased, respectively, by orders with respected to the current available ones. The unavoidable wide energy spread ($\sim$300 MeV) could be remedied by postacceleration, e.g., to less than 0.1% at 500 GeV. Moreover, the positron beam has a high flux up to $\sim 10^{19} e^+$/s thanks to the ultrashort duration ($L_e \simeq 20$ fs), which is favorable for a probe [71] along with a potential for ultrafast diagnosis.

*liyanfei@xjtu.edu.cn
†yueyuechen@shnu.edu.cn
‡huasi_hu@mail.xjtu.edu.cn

[1] D. W. Gidley, A. R. Köymen, and T. W. Capehart, Polarized Low-Energy Positrons: A New Probe of Surface Magnetism, Phys. Rev. Lett. **49,** 1779 (1982).

[2] J. Van House and P. W. Zitzewitz, Probing the positron moderation process using high-intensity, highly polarized slow-positron beams, Phys. Rev. A **29,** 96 (1984).

[3] A. Rich, J. Van House, D. W. Gidley, and R. S. Conti, Spin-polarized low-energy positron beams and their applications, Appl. Phys. A **43**, 275 (1987).

[4] L. Elouadrhiri, T. A. Forest, J. Grames, W. Melnitchouk, and E. Voutier, Proceedings of the international workshop on positrons at Jefferson lab, AIP Conf. Proc. **1160**, 13 (2009), https://aip.scitation.org/toc/apc/1160/1.

[5] A. V. Subashiev, Yu. A. Mamaev, Yu. P. Yashin, and J. E. Clendenin, Spin polarized electrons: Generation and applications, Phys. Low Dimens. Struct. **1**,1 (1998) [SLAC PUB 8035 (1998)], https://www-public.slac.stanford.edu/sciDoc/docMeta.aspx?slacPubNumber=SLAC-PUB-8035.

[6] G. Moortgat-Pick *et al.*, Polarized positrons and electrons at the linear collider, Phys. Rep. **460**, 131 (2008).

[7] T. Behnke, J. E. Brau, B. Foster, J. Fuster, M. Harrison, J. McEwan Paterson, M. Peskin, M. Stanitzki, N. Walker, and H. Yamamoto, The international linear collider technical design report–Volume 1: Executive summary, arXiv:1306.6327.

[8] K. Flottman, Investigations toward the development of polarized and unpolarized high intensity positron sources for linear colliders, Report No. DESY 93-161, 1993.

[9] P. W. Zitzewitz, J. C. Van House, A. Rich, and D. W. Gidley, Spin Polarization of Low-Energy Positron Beams, Phys. Rev. Lett. **43**, 1281 (1979).

[10] A. A. Sokolov and I. M. Ternov, On polarization and spin effects in the theory of synchrotron radiation, Sov. Phys. Dokl. **8**, 1203 (1964).

[11] T. Omori, M. Fukuda, T. Hirose, Y. Kurihara, R. Kuroda, M. Nomura, A. Ohashi, T. Okugi, K. Sakaue, T. Saito, J. Urakawa, M. Washio, and I. Yamazaki, Efficient Propagation of Polarization from Laser Photons to Positrons through Compton Scattering and Electron-Positron Pair Creation, Phys. Rev. Lett. **96**, 114801 (2006).

[12] G. Alexander *et al.*, Observation of Polarized Positrons from an Undulator-Based Source, Phys. Rev. Lett. **100**, 210801 (2008).

[13] D. Abbott *et al.* (PEPPo Collaboration), Production of Highly Polarized Positrons Using Polarized Electrons at MeV Energies, Phys. Rev. Lett. **116**, 214801 (2016).

[14] S. Corde, K. Ta Phuoc, G. Lambert, R. Fitour, V. Malka, A. Rousse, A. Beck, and E. Lefebvre, Femtosecond x rays from laser-plasma accelerators, Rev. Mod. Phys. **85**, 1 (2013).

[15] A. P. Potylitsin, Production of polarized positrons through interaction of longitudinally polarized electrons with thin targets, Nucl. Instrum. Methods Phys. Res., Sect. A **398**, 395 (1997).

[16] W. H. McMaster, Matrix representation of polarization, Rev. Mod. Phys. **33**, 8 (1961).

[17] V. A. Baskov, Radiation length of the oriented crystal, Bulletin of the Lebedev Physics Institute **42**, 144 (2015).

[18] H. Olsen and L. C. Maximon, Photon and electron polarization in high-energy bremsstrahlung and pair production with screening, Phys. Rev. **114**, 887 (1959).

[19] J. C. Liu, T. Kotseroglou, W. R. Nelson, and D. Schultz, Polarization study for the NLC Positron Source using EGS4, Report No. SLAC-PUB-8477, 2000.

[20] J. W. Yoon, C. Jeon, J. Shin, S. K Lee, H. W. Lee, I. W. Choi, H. T. Kim, J. H. Sung, and C. H. Nam, Achieving the laser intensity of 5.5×10^{22} w/cm² with a wavefront-corrected multi-PW laser, Opt. Exp. **27**, 20412 (2019).

[21] M. Wen, M. Tamburini, and C. H. Keitel, Polarized Laser-Wakefield-Accelerated Kiloampere Electron Beams, Phys. Rev. Lett. **122**, 214801 (2019).

[22] Y.-F. Li, R. Shaisultanov, K. Z. Hatsagortsyan, F. Wan, C. H. Keitel, and J.-X. Li, Ultrarelativistic Electron-Beam Polarization in Single-Shot Interaction with an Ultraintense Laser Pulse, Phys. Rev. Lett. **122**, 154801 (2019).

[23] D. Seipt, D. Del Sorbo, C. P. Ridgers, and A. G. R. Thomas, Ultrafast polarization of an electron beam in an intense bichromatic laser field, Phys. Rev. A **100**, 061402(R) (2019).

[24] Y. Wu, L. Ji, X. Geng, Q. Yu, N. Wang, B. Feng, Z. Guo, W. Wang, C. Qin, X. Yan, L. Zhang, J. Thomas, A. Hützen, A. Pukhov, M. Büscher, B. Shen, and R. Li, Polarized electron acceleration in beam-driven plasma wakefield based on density down-ramp injection, Phys. Rev. E **100**, 043202 (2019).

[25] H.-H. Song, W.-M. Wang, J.-X. Li, Y.-F. Li, and Y.-T. Li, Spin-polarization effects of an ultrarelativistic electron beam in an ultraintense two-color laser pulse, Phys. Rev. A **100**, 033407 (2019).

[26] Y.-F. Li, R. Shaisultanov, Y.-Y. Chen, F. Wan, K. Z. Hatsagortsyan, C. H. Keitel, and J.-X.Li, Polarized Ultrashort Brilliant Multi-Gev γ Rays via Single-Shot Laser-Electron Interaction, Phys. Rev. Lett. **124**, 014801 (2020).

[27] Y.-Y. Chen, P.-L. He, R. Shaisultanov, K. Z. Hatsagortsyan, and C. H. Keitel, Polarized Positron Beams via Intense Two-Color Laser Pulses, Phys. Rev. Lett. **123**, 174801 (2019).

[28] F. Wan, R. Shaisultanov, Y.-F. Li, K. Z. Hatsagortsyan, C. H. Keitel, and J.-X. Li, Ultrarelativistic polarized positron jets via collision of electron and ultraintense laser beams, Phys. Lett. B **800**, 135120 (2020).

[29] B. King and N. Elkina, Vacuum birefringence in high-energy laser-electron collisions, Phys. Rev. A **94**, 062102 (2016).

[30] D. Del Sorbo, D. Seipt, T. G. Blackburn, A. G. R. Thomas, C. D. Murphy, J. G. Kirk, and C. P. Ridgers, Spin polarization of electrons by ultraintense lasers, Phys. Rev. A **96**, 043407 (2017).

[31] E. Esarey, C. B. Schroeder, and W. P. Leemans, Physics of laser-driven plasma-based electron accelerators, Rev. Mod. Phys. **81**, 1229 (2009).

[32] G. A. Mourou, T. Tajima, and S. V. Bulanov, Optics in the relativistic regime, Rev. Mod. Phys. **78**, 309 (2006).

[33] A. Macchi, M. Borghesi, and M. Passoni, Ion acceleration by superintense laser-plasma interaction, Rev. Mod. Phys. **85**, 751 (2013).

[34] J. Ferri, S. Corde, A. Döpp, A. Lifschitz, A. Doche, C. Thaury, K. Ta Phuoc, B. Mahieu, I. A. Andriyash, V. Malka, and X. Davoine, High-Brilliance Betatron γ-Ray Source Powered by Laser-Accelerated Electrons, Phys. Rev. Lett. **120**, 254802 (2018).

[35] W.-M. Wang, Z.-M. Sheng, P. Gibbon, L.-M. Chen, Y.-T. Li, and J. Zhang, Collimated ultrabright gamma rays from electron wiggling along a petawatt laser-irradiated wire in the QED regime, Proc. Natl. Acad. Sci. U.S.A. **115**, 9911 (2018).

[36] O. Lundh, J. Lim, C. Rechatin, L. Ammoura, A. Ben-Ismal, X. Davoine, G. Gallot, J-P. Goddet, E. Lefebvre, V. Malka, and J. Faure, Few femtosecond, few kiloampere electron bunch produced by a laserplasma accelerator, Nat. Phys. 7, 219 (2011).

[37] R. Weingartner, S. Raith, A. Popp, S. Chou, J. Wenz, K. Khrennikov, M. Heigoldt, A. R. Maier, N. Kajumba, M. Fuchs, B. Zeitler, F. Krausz, S. Karsch, and F. Grüner, Ultralow emittance electron beams from a laser-wakefield accelerator, Phys. Rev. ST Accel. Beams 15, 111302 (2012).

[38] Y. Ma, J. Zhao, Y. Li, D. Li, L. Chen, J. Liu, S. J. D. Dann, Y. Ma, X. Yang, Z. Ge, Z. Sheng, and J. Zhang, Ultrahigh-charge electron beams from laser-irradiated solid surface, Proc. Natl. Acad. Sci. U.S.A. 115, 6980 (2018).

[39] X. L. Zhu, T.-P. Yu, Z.-M. Sheng, Y. Yin, I. C. Edmond Turcu, and A. Pukhov, Dense Gev electronpositron pairs generated by lasers in near-critical-density plasmas, Nat. Commun. 7, 13686 (2016).

[40] K.-H. Steffens, H. G. Andresen, J. Blume-Werry, F. Klein, K. Aulenbacher, and E. Reichert, A spin rotator for producing a longitudinally polarized electron beam with mami, Nucl. Instrum. Methods Phys. Res., Sect. A 325, 378 (1993).

[41] J. Buon and K. Steffen, Hera variable-energy mini spin rotator and head-on ep collision scheme with choice of electron helicity, Nucl. Instrum. Methods Phys. Res., Sect. A 245, 248 (1986).

[42] A. Di Piazza, C. Müller, K. Z. Hatsagortsyan, and C. H. Keitel, Extremely high-intensity laser interactions with fundamental quantum systems, Rev. Mod. Phys. 84, 1177 (2012).

[43] V. I. Ritus, Quantum effects of the interaction of elementary particles with an intense electromagnetic field, J. Sov. Laser Res. 6, 497 (1985).

[44] M. B. Plenio and P. L. Knight, The quantum-jump approach to dissipative dynamics in quantum optics, Rev. Mod. Phys. 70, 101 (1998).

[45] V. N. Baier, V. M. Katkov, and V. M. Strakhovenko, Electromagnetic Processes at High Energies in Oriented Single Crystals (World Scientific, Singapore, 1998).

[46] C. P. Ridgers, J. G. Kirk, R. Duclous, T. G. Blackburn, C. S. Brady, K. Bennett, T. D. Arber, and A. R. Bell, Modelling gamma-ray photon emission and pair production in high-intensity lasermatter interactions, J. Comput. Phys. 260, 273 (2014).

[47] N. V. Elkina, A. M. Fedotov, I. Yu. Kostyukov, M. V. Legkov, N. B. Narozhny, E. N. Nerush, and H. Ruhl, Qed cascades induced by circularly polarized laser fields, Phys. Rev. ST Accel. Beams 14, 054401 (2011).

[48] A. Gonoskov, S. Bastrakov, E. Efimenko, A. Ilderton, M. Marklund, I. Meyerov, A. Muraviev, A. Sergeev, I. Surmin, and E. Wallin, Extended particle-in-cell schemes for physics in ultrastrong laser fields: Review and developments, Phys. Rev. E 92, 023305 (2015).

[49] Users Manual of CAIN Version 2.42, http://lcdev.kek.jp/~yokoya/CAIN/.

[50] See the Supplemental Material at http://link.aps.org/supplemental/10.1103/PhysRevLett.125.044802 for details

on the applied theoretical model, and simulated results for other laser and electron parameters.

[51] M. Kh. Khokonov and I. Z. Bekulova, Length of formation of processes in a constant external field at high energies, Tech. Phys. 55, 728 (2010).

[52] V. B. Berestetskii, E. M. Lifshitz, and L. P. Pitaevskii, Quantum Electrodynamics (Pergamon, Oxford, 1982).

[53] B. King, N. Elkina, and H. Ruhl, Photon polarization in electron-seeded pair-creation cascades, Phys. Rev. A 87, 042117 (2013).

[54] F. Wan, Y. Wang, R.-T. Guo, Y.-Y. Chen, R. Shaisultanov, Z.-F. Xu, K. Z. Hatsagortsyan, C. H. Keitel, and J.-X. Li, High-energy γ-photon polarization in nonlinear breit-wheeler pair production and γ-polarimetry, arXiv:2002.10346.

[55] V. Bargmann, Louis Michel, and V. L. Telegdi, Precession of the Polarization of Particles Moving in a Homogeneous Electromagnetic Field, Phys. Rev. Lett. 2, 435 (1959).

[56] V. N. Baier, Radiative polarization of electrons in storage rings, Sov. Phys. Usp. 14, 695 (1972).

[57] A. R. Bell and J. G. Kirk, Possibility of Prolific Pair Production with High-Power Lasers, Phys. Rev. Lett. 101, 200403 (2008).

[58] Y. I. Salamin, G. R. Mocken, and C. H. Keitel, Electron scattering and acceleration by a tightly focused laser beam, Phys. Rev. ST Accel. Beams 5, 101301 (2002).

[59] A. J. Gonsalves et al., Petawatt Laser Guiding and Electron Beam Acceleration to 8 Gev in a Laser-Heated Capillary Discharge Waveguide, Phys. Rev. Lett. 122, 084801 (2019).

[60] W. P. Leemans, A. J. Gonsalves, H.-S. Mao, K. Nakamura, C. Benedetti, C. B. Schroeder, C. Tóth, J. Daniels, D. E. Mittelberger, S. S. Bulanov, J.-L. Vay, C. G. R. Geddes, and E. Esarey, Multi-Gev Electron Beams from Capillary-Discharge-Guided Subpetawatt Laser Pulses in the Self-Trapping regime, Phys. Rev. Lett. 113, 245002 (2014).

[61] C. B. Schroeder, E. Esarey, C. G. R. Geddes, C. Benedetti, and W. P. Leemans, Physics considerations for laser-plasma linear colliders, Phys. Rev. ST Accel. Beams 13, 101301 (2010).

[62] D. R. Nicholson, Introduction to Plasma Theory (Krieger, Malabar, FL, 1992).

[63] C. Sun, J. Zhang, J. Li, W. Z. Wu, S. F. Mikhailov, V. G. Popov, H. L. Xu, A. W. Chao, and Y. K. Wu, Polarization measurement of stored electron beam using touschek lifetime, Nucl. Instrum. Methods Phys. Res., Sect. A 614, 339 (2010).

[64] Jefferson Lab, https://www.jlab.org/.

[65] R. Dollan, K. Laihem, and A. Sch'alicke, Monte-carlo-based studies of a polarized positron source for international linear collider (ILC), Nucl. Instrum. Methods Phys. Res., Sect. A 559, 185 (2006).

[66] S. Riemann, F. Staufenbiel, G. Moortgat-Pick, and A. Ushakov, Photon collimator system for the ILC positron source, arXiv:1412.2498.

[67] A. Drozhdin, Y. Nosochkov, and F. Zhou, Beam collimation studies for the ILC positron source, EPAC08, Genoa, Italy (Stanford Linear Accelerator Center (SLAC), Menlo Park, 2008), https://digital.library.unt.edu/ark:/67531/metadc897949/.

[68] X. Artru, R. Chehab, M. Chevallier, V. M. Strakhovenko, A. Variola, and A. Vivoli, Polarized and unpolarized positron sources for electronpositron colliders, Nucl. Instrum. Methods Phys. Res., Sect. B **266,** 3868 (2008).

[69] R. Budny, Weak effects in annihilations producing spin-1/2 and spin-0 particle pairs, Phys. Rev. D **14,** 2969 (1976).

[70] SLAC Sit Office, Technical design report for the FACET-II project at SLAC national accelerator laboratory, Report No. SLAC-R-1072, 2016.

[71] N. Djourelov, A. Oprisa, and V. Leca, Project for a source of polarized slow positrons at ELI-NP, in *Positron Annihilation —ICPA-17*, Defect and Diffusion Forum Vol. 373 (Trans Tech Publications Ltd, Switzerland, 2017), pp. 57–60.